Journal of Colloid and Interface Science 375 (2012) 187–192

Contents lists available at SciVerse ScienceDirect

Journal of Colloid and Interface Science

www.elsevier.com/locate/jcis

Comparison of residual oil cluster size distribution, morphology and saturation in oil-wet and water-wet sandstone

S. Iglauer [a,*], M.A. Fernø [b,1], P. Shearing [c,2], M.J. Blunt [d,3]

[a] Curtin University, Department of Petroleum Engineering, 26 Dick Perry Avenue, 6151 Kensington, Australia
[b] University of Bergen, Department of Physics and Technology, Allégaten 55, 5007 Bergen, Norway
[c] University College London, Department of Chemical Engineering, Torrington Place, WC1E 7JE London, United Kingdom
[d] Imperial College London, Department of Earth Science and Engineering, Prince Consort Road, SW7 2AZ London, United Kingdom

ARTICLE INFO

Article history:
Received 23 December 2011
Accepted 14 February 2012
Available online 23 February 2012

Keywords:
Residual trapping
Residual oil saturation
Oil-wet
X-ray micro-tomography

ABSTRACT

We imaged an oil-wet sandstone at residual oil saturation (S_{or}) conditions using X-ray micro-tomography with a nominal voxel size of $(9\ \mu m)^3$ and monochromatic light from a synchrotron source. The sandstone was rendered oil-wet by ageing with a North Sea crude oil to represent a typical wettability encountered in hydrocarbon reservoirs. We measured a significantly lower S_{or} for the oil-wet core (18.8%) than for an analogue water-wet core (35%). We analysed the residual oil cluster size distribution and find consistency with percolation theory that predicts a power-law cluster size distribution. We measure a power-law exponent $\tau = 2.12$ for the oil-wet core which is higher than τ for the water-wet system ($\tau = 2.05$), indicating fewer large clusters in the oil-wet case. The clusters are rough and sheet-like consistent with connectivity established through layers in the pore space and occupancy of the smaller pores; in contrast the clusters for water-wet media occupy the centres of the larger pores. These results imply less trapping of oil, but with a greater surface area for dissolution. In carbon storage applications, this suggests that in CO_2-wet systems, capillary trapping is less significant, but that there is a large surface area for dissolution and reaction.

1. Introduction

The displacement of a fluid in a porous medium by a second immiscible or partially miscible fluid is a fundamental process which is relevant for many technological applications. Possible driving forces for such a two-phase displacement process can be externally applied viscous or gravity forces which push the displacing fluid through the porous medium. A residual phase of the displaced fluid remains in the porous medium. This residual phase can be advantageous such as in carbon geo-sequestration, where residual trapping of displaced CO_2 could ensure long-term storage [1,2], or it can be a significant problem, in, for instance, waterflooding for oil recovery, where large volumes of oil can remain in the subsurface and cannot be produced (the residual oil saturation, [3]). Another example where a residual phase is problematic is an aquifer contaminated by hazardous industrial non-aqueous solvents which cannot be completely removed from the subsurface through displacement with water or other immiscible fluids. It is important to understand the characteristics of the residual phase, including saturation, cluster size distribution, and cluster morphology to aid the design of improved oil and pollutant recovery, and ensure secure CO_2 storage.

Specifically, the residual CO_2 saturation determines the effectiveness and capacity of the residual trapping mechanism in carbon geo-sequestration projects [4,5], while the cluster size distribution and interfacial CO_2-brine areas affect the rate of CO_2 dissolution in formation brine (dissolution trapping [6]). Smaller CO_2 clusters dissolve faster in brine, which accelerates dissolution trapping [7,8] and subsequently mineral trapping when the species in the carbonated brine react with themselves or the host rock [9].

The residual phase saturation is a complex function of the pore morphology of the porous medium, the fluid–fluid interfacial tension and the solid-fluid-fluid contact angle distribution [10,11]. The trapping of oil and CO_2 has been measured in core-scale (cm) experiments, but these do not reveal the pore-scale distribution of trapped clusters (see, for instance [5,12]).

Recently X-ray micro-computed tomography (μ-CT) has been used to image the rock and resident fluids at the pore (μm) scale. Several researchers have imaged residual saturations in porous media [13–20]. In previous work [14,15], the cluster size distributions of oil (n-octane) and super-critical CO_2 trapped by brine were compared for water-wet Doddington sandstone. Clusters of all size

* Corresponding author. Tel.: +61 8 9266 7703.
E-mail address: stefan.iglauer@curtin.edu.au (S. Iglauer).
[1] Tel.: +47 55 58 27 92.
[2] Tel.: +44 207 679 3783.
[3] Tel.: +44 020 7594 6500.

0021-9797
http://dx.doi.org/10.1016/j.jcis.2012.02.025

were observed, with approximately power-law distributions. Less trapping of CO_2 was seen, consistent with core-scale experiments, that was interpreted as an indication of weakly water-wet conditions [5]. For CO_2, fewer small trapped clusters and more large clusters were present, compared to trapping of oil in a strongly water-wet system.

Most oil reservoirs are not water-wet, but display oil-wet or mixed-wet conditions due principally to the sorption of complex, surface-active compounds in the crude oil to the rock surface [21–23]. In a CO_2 context, organic contaminants or clays may result in effectively CO_2-wet conditions. Furthermore, CO_2 storage may be implemented in mature oil fields [24], where it is likely – for the reasons above – that CO_2-wet conditions will be encountered, as observed directly in contact angle measurements [25].

Al-Raoush [18] studied the distribution of trapped oil in bead packs as the fraction of oil-wet beads was changed. The clusters became smaller with more oil-wet conditions. Landry et al. [19] compared trapping for water-wet and oil-wet bead packs and measured interfacial areas. They too observed that there were more small clusters under oil-wet conditions. In these two studies, wettability was altered by using acrylic plastic beads and the porous medium itself was not necessarily representative of consolidated reservoir rocks. Kumar et al. [20] investigated the residual oil phase in a mixed-wet dolomite core and found only a slightly reduced S_{or} (32%) when compared to an analogue water-wet sample (S_{or} = 35%). Their mixed-wet core was prepared with a stearic-acid in heptane solution which may not be representative of crude oil, that has a significantly more complex composition. It is possible that this core was still weakly water-wet after treatment.

In this paper, we age a sandstone in crude oil to reproduce the likely wettability alteration observed in oil reservoirs, and study the morphology and cluster-size distribution of trapped clusters. We compare with measurements on an unaltered, water-wet rock. We only consider the trapping of oil and do not study three-phase (oil, brine and gas, or CO_2) systems.

2. Materials and methods

The properties of the fluids used in this study are listed in Table 1. n-decane was used as the oil phase and brine doped with 10 wt% potassium iodide (to enhance CT contrast) was the aqueous phase. A North Sea reservoir crude oil (composition is shown in Table 2) was used to render the surface of the sandstone contacted by crude oil-wet (ageing). The ageing process is described in detail below. After ageing, the crude oil was miscibly displaced from the pore space by decahydronaphtahlene followed by n-decane.

The SARA (Saturates, Aromatics, Resins and Asphaltenes) components in the crude (Table 2) were measured using standard HPLC methods [26]. The procedure is outlined below:

Preparation. 1 g crude oil was mixed with 36 ml n-hexane to force asphaltene precipitation. 3 ml maltenes were extracted from the top, without disturbing the precipitated asphaltenes, and placed in a new bottle.

Saturates and aromatics. 25 μl maltenes were injected into a LC-20AT prominence liquid chromatograph (Shimazu) to evaluate presences of saturates and aromatics with a single ring and two rings, respectively.

Resins. 2.5 ml oil and n-hexane mixture were introduced to a LC-20AT prominence liquid chromatograph with a μBondpak NH2 column mounted in the system. The resins were adsorbed in the cell due to its polarity. The resins were flushed out of the column, collected in clean bottles and weighed to quantify the amount of resin.

Asphaltenes. The remaining oil and n-hexane mixture, with asphaltene precipitation, was filtered through small filters with the aid of a vacuum pump, and allowed to dry overnight. The amount of asphaltene was quantified by mass measurement.

A clean, well sorted, relatively homogeneous sandstone outcrop (Clashach) was used in this study. Clashach is a quarried sandstone from Elgin in Scotland (located close to Aberdeen); petrophysical and petrochemical properties of Clashach are displayed in Table 3. Cylindrical sandstone plugs were drilled with a diameter of 5 mm and lengths 10–15 mm.

The cores were housed in flow cells which were designed to perform at both room temperature and ageing temperature (353 K = 80 °C). Each cell consisted of metal end pieces, polyester heat shrink tubing (curing temperature 473 K = 200 °C) and a two component epoxy resin, Fig. 1. The epoxy layers were cut on a lathe to create a smooth cylindrical surface (which results in better micro-tomography (μ-CT) images).

Wettability alteration. The core plug in the flow cell was saturated with doped brine under vacuum (<100 Pa). The flow cell was then placed in an oven (353 K) at ambient pressure and crude oil was injected through the core plug. The crude oil was previously filtered through a chalk filter to remove impurities [28].

During ageing, crude oil was injected through the core plug at a constant injection rate (5 ml/hr; this corresponds to a capillary number $N_{cap} = v\mu/\sigma = 3.8 \times 10^{-4}$) to displace brine from the pore space and establish connate water saturation (S_{wc}) during primary drainage. The injection rate was reduced to 1 ml/hr when brine production stopped and S_{wc} was reached. The small fluid volumes made it difficult to accurately measure the average water saturation at S_{wc} via mass balance; we assume that S_{wc} in the small core is equal to the S_{wc} in the larger core (=0.44), see details below. Fresh crude oil was continuously supplied to the cores to enhance the wettability alteration process [29]. The flow of crude oil through the cores was periodically stopped during ageing to reduce the effect of a flowing crude oil on slow rock/brine/crude oil interactions. The direction of flow was reversed after 5 days, with a total ageing time of 10 days. After ageing, the crude oil was miscibly displaced from the core by injecting more than 5 PV (pore volumes) of decahydronaphthalene followed by 5 PV of n-decane. Decahydronaphthalene was injected to avoid direct contact between crude oil and n-decane to reduce asphaltene precipitation [30]. n-decane was used as the oil phase after ageing to avoid further ageing by the crude oil, to improve the reproducibility and to simplify the oil chemistry [31,32]. After ageing and crude oil exchange by n-decane, the oven was turned off and the core plug

Table 1
Fluid properties.

Fluid	Density @ 293 K (kg/m^3)	Density @ 353 K (kg/m^3)	Viscosity @ 293 K (mPa s)	Viscosity @ 353 K (mPa s)
Brine (10 wt% KI)	1030		1.07	
n-Decane	730	680	0.92	0.40
Decahydronaphthalene	890	–	0.85	–
Crude oil	850	850	14.3	2.7

Table 2
Crude oil composition.

Acid number	Base number	Refractive index	Mass% saturates	Mass% aromatics	Mass% resins	Mass% asphaltenes
0.41 ± 0.02	1.4 ± 0.1	1.4834	61 ± 3	20 ± 1	19 ± 1	0.59 ± 0.03

Table 3
Petrophysical and petrochemical properties of Clashach sandstone.

Sandstone	Porosity	Brine permeability (m^2)	Surface area[a] (m^2/g)	Chemical composition[b] (wt%)
Clashach	0.144	9.6×10^{-14}	0.37	α-quartz 96 K-feldspar 2 Calcite 1 Ankerite ~1 Illite trace

[a] [27].
[b] Measured via X-ray diffraction on a Philips PW1830 diffractometer.

was cooled to room temperature for at least 24 h. The core plug was then waterflooded with 10 PV of brine at a capillary number of 10^{-7}; we assume that analogous to the large core (see below) this established a uniform residual oil saturation (S_{or}). We assume that this leaves the minimum, disconnected oil saturation. However, as we discuss later, the oil may continue to drain slowly through oil layers with continued waterflooding.

To quantify the wettability of the aged cores, an independent Amott experiment [33] was conducted on a separate larger sample (diameter = 38.1 mm, length = 76.6 mm) which was aged in the same way as the small core. The core was oil-flooded to $S_{wc} = 0.44$ and immersed in brine in a glass cell at ambient conditions; spontaneous imbibition of brine into the core was measured over 1000 h. No oil was produced and no brine spontaneously imbibed into the core. The core plug was then waterflooded with 50 PV of brine at a capillary number of 10^{-7} to establish residual oil saturation. No oil production was observed visually after injection of 1–2 PV of brine; S_{or} was measured to be 11%. This is lower than measured from the μ-CT experiment, 18.8%, where less water was injected. This could be due to continued oil layer drainage in this experiment, or differences in the averaged behaviour of the two cores, which are of different size. This is discussed further later in the paper. The core was then placed in an inverted glass cell filled with oil to measure the spontaneous imbibition of oil. Produced water as a function of time was measured for 1000 h (41 days). The core plug was then oil-flooded with 50 PV of oil at a capillary number of 10^{-7} to establish connate water saturation. The endpoint water saturations after each process were used to calculate the Amott water and oil indices (the fraction of the total change in saturation achieved by imbibition) $I_w = 0$ and $I_o = -0.1$. The calculated Amott-Harvey index [33] for the aged core was $I_{A-H} = I_w - I_o = -0.1$. A negative I_{A-H} index indicates oil-wet conditions, and the interval [−0.3; −0.1] is classified as weakly oil-wet [19]. The core investigated here is therefore weakly oil-wet.

A μ-CT image of the small core at S_{or} conditions was then acquired using monochromatic X-rays (30 keV photon energy) at the SYRMEP beamlime (Elettra light source, Trieste, Italy). The obtained μ-CT images were cleaned of ring artefacts [34], filtered with an anisotropic regularisation filter [35] and segmented with a multi-thresholding method based on Otsu's algorithm [36] (Fig. 2).

3. Results and discussion

We measured porosity and residual oil saturation on the μ-CT images, Tables 3 and 4; the μ-CT porosity value was consistent with an independent porosity measurement using Helium pycnometry [14]. S_{or} in the oil-wet core (18.8%) was lower than the S_{or} in an analogous water-wet system (35%), Table 4; this is consistent with larger scale core floods cited in the literature [11] and S_{or} measured on the larger core for the Amott test (= 11%). As mentioned previously, the lower S_{or} value in the Amott test may be a consequence of the larger number of PV of brine injected. In an oil-wet system, oil layers, sandwiched between water remaining in the corners of the pore space and water in the centre, retain connectivity of the oil phase, allowing, slowly, low residual saturations to be achieved, with the remaining oil saturation declining with PV injected – this is consistent with the lower Amott test S_{or} [11]. This behaviour is reflected in the shape and locations of the residual oil clusters. In the oil-wet case, the trapped oil is located close to the solid surface (in layers) or occupies the smaller pores (see Fig. 2b). The largest clusters span many pores, consistent with connectivity through layers and smaller pores, since the structures are thin, resembling crumpled sheets (Fig. 3a and b). The water-wet case is very different [14], with oil occupying the centres of the larger pores. The smallest clusters are broadly spherical in shape, centred in a single pore, while the larger clusters – see Fig. 3c – are overall fatter and reflect the connectivity of the widest pore spaces. The behaviour is also distinctly different in a super-critical CO_2-brine system. S_r (the residual phase here is CO_2) is lower – around 25% – but there are fewer small clusters and more large ones; specifically we measured a power-law cluster size distribution exponent of 2.01 [15]. This is interpreted as the CO_2 being only weakly

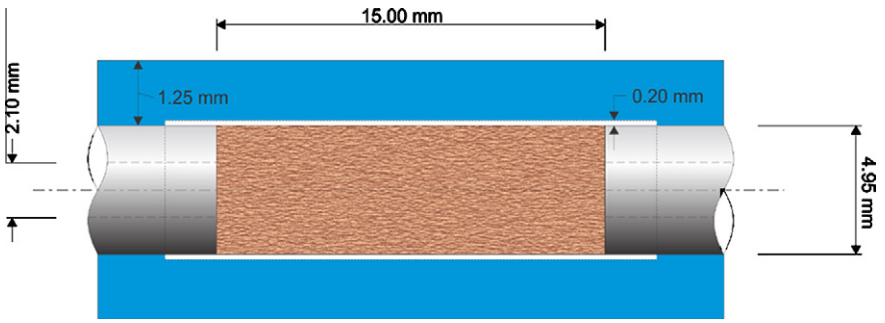

Fig. 1. Flow cell for fluid injection during wettability alteration and waterflooding of core plugs imaged using X-ray micro-tomography. The core (yellow–brown) has a diameter of 5 mm and a length of 15 mm. The white tube is the polyester heat shrink sleeve and the blue volume is the epoxy resin. To the left and right are the stainless steel inlet and outlet pieces (not shown completely).

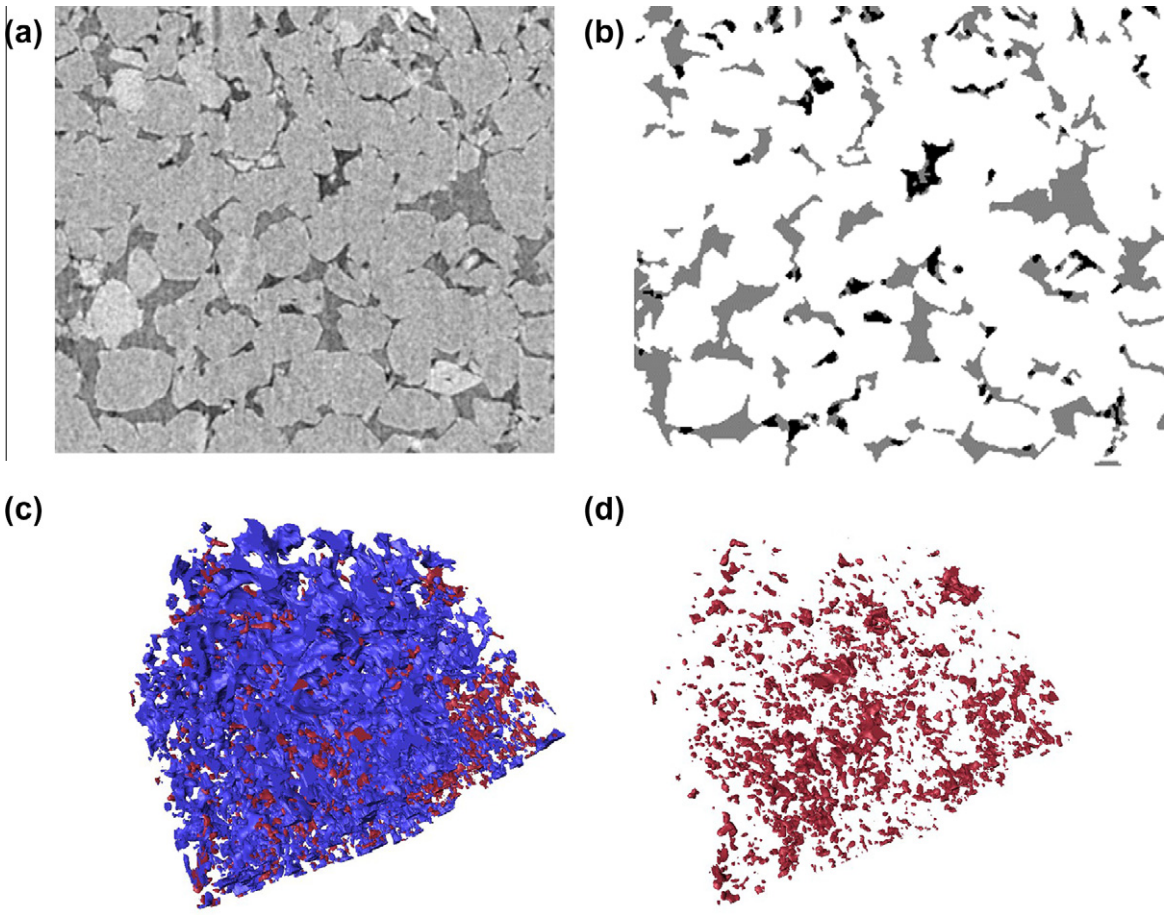

Fig. 2. Images showing the oil-wet core after waterflooding (nominal voxel size was (9 μm)^3): (a) two-dimensional slice through the core; oil is black, brine dark grey and rock light grey. The area displayed is 2.7 mm × 2.7 mm = 7.29 mm^2 (300 × 300 pixels), (b) the same image segmented; oil is black, brine dark grey and rock is white, (c) residual oil clusters (red) and surrounding brine (blue) in three dimensions; the volume displayed is 2.808 mm × 3.222 mm × 2.88 mm ≈ 26.06 mm^3 (312 × 358 × 320 voxels), and (d) Residual oil clusters (red) in three dimensions; the volume displayed is also 312 × 358 × 320 voxels.

Table 4
Residual oil cluster statistics in water-wet and oil-wet Clashach sandstone.

Water-wet			Oil-wet	
S_{or} measured via μ-CT[a]	S_{or} measured via core flood[b]	τ[a]	S_{or} measured via μ-CT	τ
0.35	≈0.37	2.05	0.188	2.12

[a] [14].
[b] [40].

non-wetting: this suppresses snap-off (see below) leading to fewer small stranded clusters. In this case, the CO_2 is still the non-wetting phase and so preferentially resides in the centres of the large pores. Hence S_{or} alone does not predict the cluster size distribution.

We then counted the number N of residual oil clusters of size s (in voxels). We define the cumulative cluster size distribution $S(s) = \sum_s^\infty sn(s) \propto s^{-\tau+2}$ [37] where $n(s) = N(s)/N_\upsilon$ and N_υ is the total number of pore-space voxels. Percolation theory predicts that the number N of disconnected clusters of size s scales as $N \propto s^{-\tau}$ [38] with $\tau = 2.189$ [39]. We plot $S(s)$ ($S(1)$ is the residual saturation) and $n(s)$ versus s on logarithmic axes. With the best fit to the data we obtain $\tau = 2.12$, which is higher than in the water-wet case ($\tau = 2.05$; which was measured for two different sandstone outcrops, Clashach and Doddington [14]), Table 4 and Fig. 4. We find clusters of all size, from those occupying single pores (s around 10 voxels) to clusters that span the system (s around 10,000). The difference in the values of τ indicates that there are fewer large clusters in the oil-wet case, consistent with other studies [18,19].

In water-wet media, trapping is controlled by snap-off, where water spontaneously fills the narrow regions of the pore space stranding the non-wetting phase (oil) in the larger pores [41]. In oil-wet rocks, oil remains connected through layers and will continue to drain until very low saturations are reached [42]: in our experiments we imaged the saturation distribution after 10 PV of water had been injected which may not represent a truly residual or disconnected saturation. We cannot image features smaller than 9 μm, which means that many of the thinner oil layers cannot be directly observed. As a consequence, clusters that we identify as isolated may be connected through thin layers below the resolution of the scanning.

4. Conclusions

We have presented μ-CT measurements of the residual oil saturation, residual cluster size distribution and cluster morphologies in an oil-wet sandstone, we observed a significantly lower oil saturation in the oil-wet core (18.8%) than in an analogue water-wet sandstone (35%, [14]), or in a CO_2/brine/sandstone system (25%, [15]). This is consistent with core-scale measurements [4,5,11,12,43].

We observed that the residual cluster morphologies in the oil-wet sandstone were significantly different to those observed in

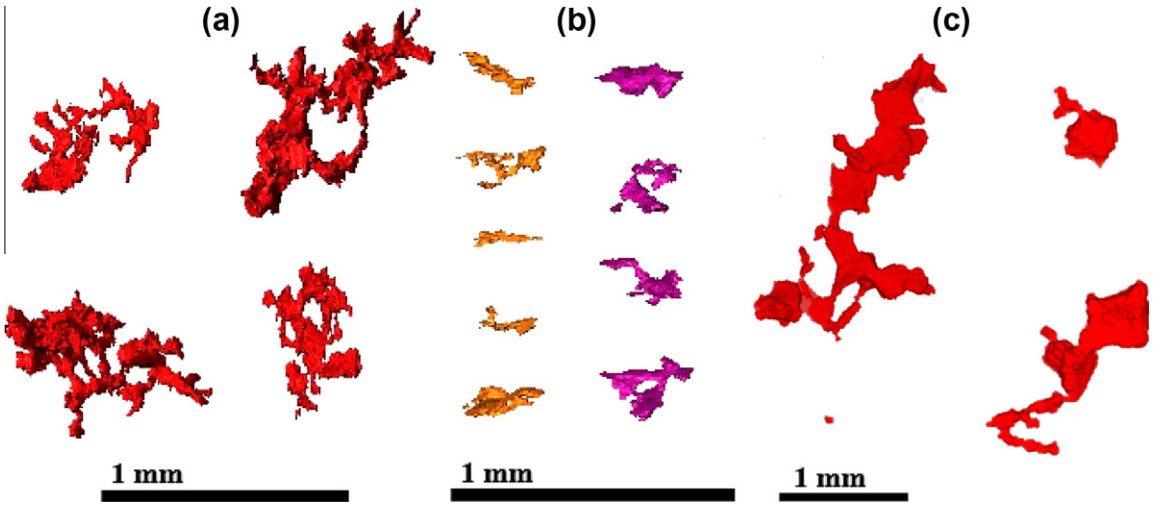

Fig. 3. (a) The four largest residual oil clusters in the oil-wet sandstone (size 10917–15653 voxels), (b) medium sized residual oil clusters (purple = 1000–1100 voxels and orange = 500–600 voxels) in the oil-wet sandstone, and (c) residual oil clusters in water-wet sandstone; the largest cluster has a volume of 25193 voxels [14]. The residual clusters in the oil-wet rock have a flatter sheet-like structure, in layers and filling small pores, while the clusters in water-wet rock occupy the centres of the wider pore spaces.

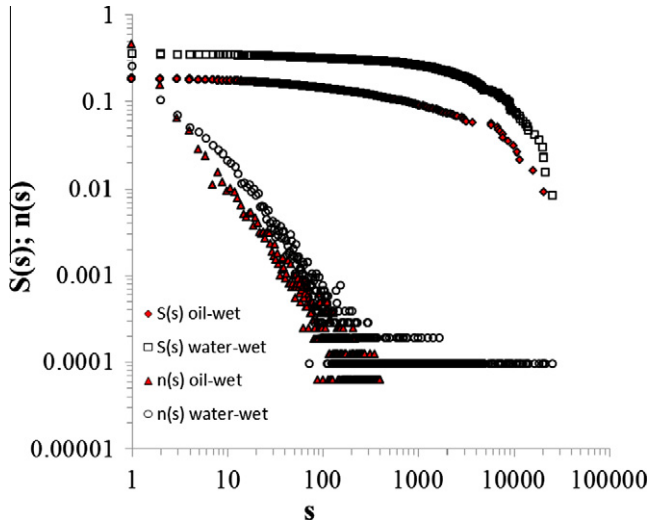

Fig. 4. Residual oil cluster distributions in water-wet and oil-wet Clashach sandstone. $S(s)$ is the cumulative, measuring the fraction of the pore space occupied by clusters of size s or larger, while $n(s)$ is the normalised cluster size distribution. s is the cluster size measured in voxels.

the water-wet case; in the oil-wet rock the residual clusters had a distinctly sheet-like flat geometry, while in the water-wet sample the residual clusters were more spherical. The residual clusters in the oil-wet sandstone were mostly located adjacent to the rock surface and more frequently in smaller pores, while in the water-wet rock these clusters were located in the middle of the larger pores. These findings can be explained using previous theoretical and micro-model analysis of the effects of contact angle on the pore-scale configurations of fluid [23,41].

In terms of cluster size distribution we measured a higher power-law cluster size distribution exponent τ (=2.12) in the oil-wet system than in the water-wet system (τ = 2.05) or a CO_2/brine system (τ = 2.01), which indicates that there are more small clusters in the oil-wet case, as seen previously in bead pack experiments [18,19].

The broad cluster size distribution implies: (a) a large surface area for dissolution (and reaction in the case of CO_2), especially when the likely effect of layers is taken into account; (b) that in carbon geo-sequestration applications less CO_2 will be trapped in CO_2-wet systems by the residual trapping mechanism; (c) an improved oil recovery from oil-wet reservoirs if significant volumes of water are injected; and (d) a potentially improved clean-up efficiency of industrial non-aqueous solvents in oil-wet formations.

Acknowledgments

We would like to thank our sponsor Shell under the Shell-Imperial Grand Challenge on Clean Fossil Fuels, and the Elettra Light Source in Trieste, Italy, for technical support and providing beamtime. We would like to thank Ahmadreza Younessi for preparing Fig. 1. PS acknowledges financial support of the Royal Academy of Engineering.

References

[1] B. Metz, O. Davidson, H. de Coninck, M. Loos, L. Meyer (Eds.), Intergovernmental Panel on Climate Change Special Report on Carbon Dioxide Capture and Storage, Cambridge University Press, 2005.
[2] R. Juanes, E.J. Spiteri, F.M. Orr, M.J. Blunt, Water Resour. Res. 42 (2006) W12418.
[3] W. Green, G.P. Willhite, Enhanced Oil Recovery, SPE Publications, Richardson, 1998.
[4] S. Iglauer, W. Wülling, C.H. Pentland, S. Al-Mansoori, M.J. Blunt, SPE J. 16 (2011) 778.
[5] C.H. Pentland, R. El-Maghraby, S. Iglauer, M.J. Blunt, Geophys. Res. Lett. 38 (2011) L06401.
[6] S. Iglauer, in: H. Nakajima (Ed.), Mass Transfer, InTech, Rijeka, 2011, pp. 233–262.
[7] S. Hirai, K. Okazaki, H. Yazawa, H. Ito, Y. Tabe, K. Hijikata, Energy 22 (1997) 363.
[8] T. Suekane, A. Mizumoto, T. Nobuso, M. Yamazaki, S. Tsushima, S. Hirai, 8th Int. Conf. Greenh. Gas Contr. Proc. (2006).
[9] I. Gaus, Int. J. Greenh. Gas Con. 4 (2010) 73.
[10] E.J. Spiteri, R. Juanes, M.J. Blunt, F.M. Orr, SPE J. 13 (2008) 277.
[11] N.R. Morrow, J. Petrol. Technol. 42 (1990) 1476.
[12] C.H. Pentland, E. Itsekiri, S. Al-Mansoori, S. Iglauer, B. Bijeljic, M.J. Blunt, SPE J. 15 (2010) 270.
[13] M. Prodanovic, W.B. Lindquist, R.S. Seright, Adv. Water Resour. 30 (2007) 214.
[14] S. Iglauer, S. Favretto, G. Spinelli, G. Schena, M.J. Blunt, Phys. Rev. E 82 (2010) 056315.
[15] S. Iglauer, A. Paluszny, C.H. Pentland, M.J. Blunt, Geophys. Res. Lett. 38 (2011) L21403.
[16] M. Kumar, T.J. Senden, A.P. Sheppard, J.P. Middleton, M. Knackstedt, Petrophys 51 (2010) 323.
[17] Z.T. Karpyn, M. Piri, G. Singh, Water Resour. Res. 47 (2011) W05511.
[18] R.I. Al-Raoush, Environ. Sci. Technol. 43 (2009) 4796–4801.

[19] C.J. Landry, Z.T. Karpyn, M. Piri, Geofluids 11 (2011) 209–227.
[20] M. Kumar, J.P. Middleton, A.P. Sheppard, T.J. Senden, M.A. Knackstedt. Int. Petr. Technol. Conf. Proc. (2009) IPTC 14001.
[21] E.C. Donaldson, W. Alam, Wettability, Gulf Publishing Company, Houston, 2008.
[22] J.S. Buckley, Y. Liu, S. Monsterleet, SPE J. 3 (1998) 54.
[23] M.J. Blunt, M.D. Jackson, M. Piri, P.H. Valvatne, Adv. Water Resour. 25 (2002) 1069.
[24] J. Moortgat, S. Sun, A. Firoozabadi, Water Resour. Res. 47 (2011) W05511.
[25] D. Yang, Y. Gu, P. Tontiwachwuthikul, Energy Fuels 22 (2008) 504.
[26] T. Fan, J.S. Buckley, Energy Fuels 16 (2002) 1571.
[27] G.P. Matthews, Powder Technol. 76 (1993) 95.
[28] M.A. Fernø, M. Torsvik, S. Haugland, A. Graue, Energy Fuels 24 (2010) 3950.
[29] A. Graue, E. Aspenes, T. Bogno, R.W. Moe, J. Ramsdal, J. Petrol. Sci. Eng. 33 (2002) 3.
[30] J.S. Buckley, Y. Liu, X. Xie, N.R. Morrow, SPE J. 2 (1997) 107.
[31] A. Graue, E. Tonheim, B.A. Baldwin, 3rd Int. Sym. Eval. Res. Wett. (1996).
[32] A. Graue, B.G. Viksund, T. Eilertsen, R. Moe, J. Petrol. Sci. Eng. 24 (1999) 85.
[33] E. Amott, Trans. Am. Inst. Min. Met. Eng. 216 (1959) 156.
[34] B. Münch, P. Trtik, F. Marone, M. Stampanoni, Opt. Express 17 (2009) 8567.
[35] D. Tschumperlé, R. Deriche, Proc. CVPR IEEE 1 (2003) 651.
[36] N. Otsu, IEEE Trans Syst. Man Cyber. 9 (1979) 62.
[37] M.M. Dias, D. Wilkinson, J. Phys. A – Math. Gen. 19 (1986) 3131.
[38] M.J. Blunt, H. Scher, Phys. Rev. E 52 (1995) 6387.
[39] C.D. Lorenz, R.M. Ziff, Phys. Rev. E 57 (1998) 230.
[40] C.H. Pentland, Y. Tanino, S. Iglauer, M.J. Blunt, SPE 133798, SPE An. Tech. Con. Proc. (2010).
[41] R. Lenormand, E. Touboul, C. Zarcone, J. Fluid Mech. 189 (1988) 165.
[42] R.A. Salathiel, J. Petrol. Technol. 25 (1973) 1216.
[43] T. Suekane, T. Nobuso, S. Hirai, M. Kiyota, Int. J. Greenh. Gas Contr. 2 (2008) 58.